GENIORS

Research and Innovation Action (RIA)

This project has received funding from the European Union's Horizon 2020 research and innovation programme under grant agreement No 755171.

Start date : 2017-06-01 Duration : 48 Months
http://geniors.eu/

studies of non- powder routes for the synthesis of MOX fuels materials, potentially bearing minor actinides and blanket fuel materials

Authors : Mr. Christian SCHREINEMACHERS (SCK-CEN), Gregory Leinders (SCK CEN), Marc Verwerft (SCK CEN), Thomas Cardinaels (SCK CEN)

GENIORS - Contract Number: 755171

Project officer: Roger Garbil

Document title	studies of non- powder routes for the synthesis of MOX fuels materials, potentially bearing minor actinides and blanket fuel materials
Author(s)	Mr. Christian SCHREINEMACHERS, Gregory Leinders (SCK CEN), Marc Verwerft (SCK CEN), Thomas Cardinaels (SCK CEN)
Number of pages	19
Document type	Deliverable
Work Package	WP4
Document number	D4.3
Issued by	SCK-CEN
Date of completion	2020-05-27 17:28:48
Dissemination level	Public

Summary

Deliverable D4.3 describes investigations on the synthesis of simulated MOX fuel particles, potentially bearing MAs and blanket materials, using the sol-gel route via internal gelation.

Approval

Date	By
2020-05-28 17:35:41	Mrs. Nicolas DACHEUX (CEA)
2020-05-29 08:35:53	Mr. Andreas GEIST (KIT)
2020-06-12 18:06:28	Mr. Stéphane BOURG (CEA)

CONTENT

This project has received funding from the EURATOM research and training programme 2014-2018 under grant agreement No 755171. The content of this deliverable reflects only the author's view. The European Commission is not responsible for any use that may be made of the information it contains.

EXECUTIVE SUMMARY

Deliverable D4.3 describes investigations on the synthesis of simulated MOX fuel particles, potentially bearing MAs and blanket materials, using the sol-gel route via internal gelation.

The sol-gel route via internal gelation was applied for the production of and Ce-doped uranium dioxide microspheres. Trivalent and tetravalent Ce precursors were used and the influence of the precursors' oxidation state on the fabrication process and the final product was studied. The successful introduction of the dopant into the $3UO_3 \cdot 2NH_3 \cdot 4H_2O$ matrix of the dried gels, independent of the dopant and the oxidation state of its precursor, was demonstrated for Ce contents up to 30mol%. Densities of the dried gels were determined and the particle volume shrinkage during the thermal treatment was investigated. X-ray powder diffraction analyses proved the presence of $U_{1-y}Ce_yO_{2\pm x}$ single phase solid solutions for the sintered Ce-doped microspheres prepared using the tetravalent precursor. For Ce-doped compositions prepared with the trivalent precursor, the presence of two solid solutions was observed for Ce contents > 15 mol%. The lattice parameters determined for the single phase solid solutions follow Vegard's law and show a decreasing lattice parameter with increasing dopant content. The conditions applied in this study allow the usage of a solution containing the gelification agents, resulting in a particle fabrication process for the production of Pu and/or minor actinide containing UO_2 transmutation fuel, which has benefits in terms of automating and remote handling, leading to a better implementation in glove boxes or hot cells.

This project has received funding from the EURATOM research and training programme 2014-2018 under grant agreement No 755171. The content of this deliverable reflects only the author's view. The European Commission is not responsible for any use that may be made of the information it contains.

FABRICATION OF $U_{Y-1}CE_YO_{2\pm X}$ SOLID SOLUTIONS

INTRODUCTION

In the context of simulated nuclear fuel materials, lanthanides act commonly as surrogates for actinides. The assignment of the surrogates based only on ionic radii, suggests using Nd^{III} (r_{CN9} = 1.161 Å) or Pr^{III} (r_{CN9} = 1.176 Å) as surrogate for Pu^{III} (r_{CN9} = 1.168 Å) [1, 2]. However, one of the most stable oxidation states of plutonium is Pu^{IV} (r_{CN8} = 0.97 Å). Cerium has the benefit of being used as Ce^{III} (r_{CN9} = 1.191 Å) and Ce^{IV} (r_{CN8} = 0.96 Å) [2]. Therefore, Ce is used to simulate Pu within this study. Besides different fabrication techniques, the suitability of trivalent and tetravalent Ce precursors are investigated for the fabrication of Ce-doped UO_2 solid solutions.

INTERNAL GELATION

Since more than six decades, sol-gel processes have been explored to avoid handling of fine powder and to facilitate automation for the production of nuclear fuel particles [3-8]. Common sol-gel methods are the routes via internal- and external gelation. Both methods are based on the precipitation of a metal nitrate solution by ammonia into a metal hydroxide, but differ amongst others in the source of ammonia. In the external gelation process, the sol is dispersed into droplets which are given into an ammonia solution, whereas in the internal gelation (IG) process, reagents are added to the sol which decompose thermally and release ammonia within droplets of the sol [9]. The resulting ammonium diuranate (ADU) particles are converted to UO_2 particles, which can directly be used as particle fuel [9] or compressed into the commonly used fuel pellets [10].

The gelation process is largely governed by the ratio (R) of the molar amounts of the gelation agents to the molar amounts of the metals. Hexamethylenetetramine (HMTA, $(CH_2)_6N_4$) and urea ($CO(NH_2)_2$) are used as gelation agents in the IG process. Depending of the metal concentration in the sol, the R ratio has to be adjusted to ensure proper gelation. A metal concentration of 1.3 mol L^{-1} and a concentration ratio R = 1.2 for both gelation agents were suggestion by Vaidya et al. [11] to form a single phase gel at gelation temperatures of 50 °C to 70 °C. Kumar et al. [12] investigated gelation parameters for the fabrication of $U_{0.47}Pu_{0.53}O_2$ particles and found R values ranging from 1.20 to 1.25 for both gelation agents suitable for a metal concentration of 1.3 mol L^{-1}, which make those conditions promising to introduce a dopant molar metal fraction up to about 50 mol%.

This project has received funding from the EURATOM research and training programme 2014-2018 under grant agreement No 755171. The content of this deliverable reflects only the author's view. The European Commission is not responsible for any use that may be made of the information it contains.

$U_{y-1}Ce_yO_{2\pm x}$ MICROSPHERES PREPARED BY INTERNAL GELATION

MATERIAL AND METHODS

PARTICLE SYNTHESIS

Figure 1 summarises schematically the individual steps of the IG process applied in this study, using an acid-deficient uranyl nitrate (ADUN) solution as uranium precursor. The fabrication of the ADUN solution (c(U) = 2.6 mol L^{-1}, pH = 1.7, ρ = 1.85 g cm^{-3}, $\frac{c(NO_3^-)}{c(UO_2^{2+})}$ = 1.56), was done by dissolving β-UO_3 in uranyl nitrate solution (UNS) as described by Haas et al. [5]. The β-UO_3 was synthesized by thermal decomposition of ADU according to the method described by Grenthe et al. [13] (pp. 341-342). A heating rate of 5 °C min^{-1} was applied to reach 450 °C and this temperature was kept for 1 h, the thermal treatment was carried out in air at ambient pressure. ADU was precipitated from a UNS via addition of a NH_3 solution.

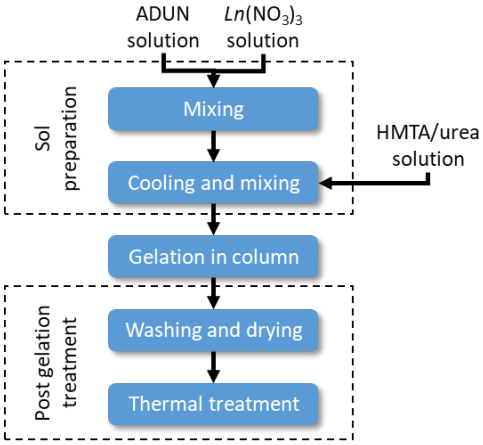

Figure 1.: Schematic overview of the IG process, studied to fabricate Ce-doped UO_2 microspheres using a trivalent Ce precursor.

PREPARATION OF AMMONIUM DIURANATE REFERENCE GELS

ADUN solution (2.0 mL) was stirred in an ice bath and a pre-cooled solution (2.0 mL) containing HMTA (3.1 mol L^{-1}) and urea (3.1 mol L^{-1}) was added, leading to c(U) = 1.3 mol L^{-1} and R = 1.2 for both gelation agents. The sol was dropped manually into a double-walled glass column filled with silicone oil (T = 90 °C) by the use of a syringe and a hollow needle (diameter = 0.45 mm). When the sol was added, the set-up was cooled to 40 °C and the gelled droplets were removed from the column to perform the post gelation treatment (Figure 1). They were

This project has received funding from the EURATOM research and training programme 2014-2018 under grant agreement No 755171. The content of this deliverable reflects only the author's view. The European Commission is not responsible for any use that may be made of the information it contains.

washed 3 times with 50 mL petroleum benzine and stored in 50 mL of ammonia solution ($w(NH_3)$ = 12.5 %). After ageing of 24 h, the particles were washed twice with 50 mL ammonia solution ($w(NH_3)$ = 12.5 %) and dried for 24 h at room temperature. Finally, the products were dried at 90 °C and a pressure of 250 mbar for 24 h.

PREPARATION OF CERIUM DOPED AMMONIUM DIURANATE GELS

The preparation of Ce-doped compositions with Ce metal fraction $\chi(Ce) = \frac{n(Ce)}{n(Ce+U)}$ varying from 5 mol% to 30 mol%, with an increment of 5 mol%, was investigated. The influence of the dopant precursors' oxidation state on the IG process and the final products was studied as well. Therefore, cerium(III)nitrate hexahydrate ($Ce(NO_3)_3 \cdot 6\,H_2O$) and diammonium cerium(IV)nitrate ($(NH_4)_2Ce(NO_3)_6$) served as dopant precursors. The trivalent precursor was dissolved in ultra pure water and a Ce molar metal concentration of 2.3 mol L^{-1} was determined via inductive coupled plasma mass spectrometry (ICP-MS).

The sol was prepared in two steps (sol preparation, Figure 1). Firstly, a metal blend solution was prepared by mixing the ADUN solution with the respective volume of the Ce nitrate solution. In the case of the tetravalent Ce precursor, $(NH_4)_2Ce(NO_3)_6$ was dissolved directly in diluted ADUN solution to end up with the desired metal ratios. Then, the metal blend solution was cooled in an ice-bath and the pre-cooled solution containing urea and HMTA was added, as described in for the un-doped material. The gelation of the sol and the post gelation treatment were also carried as described in the previous section.

THERMAL TREATMENT

The gelled particles were calcined in Al_2O_3 crucibles at 900 °C in synthetic air for 1 h, using a heating rate of 1.5 °C min^{-1} (Nabertherm, LT 9113/P330). The furnace was cooled to 150 °C with a rate of 10 °C min^{-1}, then the crucibles were placed in a desiccator to allow them to cool down to room temperature. Afterwards, the calcined particles were sintered under reducing conditions (Linn High Therm, HT-1800-Moly) in custom made Mo crucibles. Particles of each composition were heated up to 700 °C with 5 °C min^{-1} in Ar atmosphere. Then, the atmosphere was changed to a mixture of Ar:H_2 (95:5) and Ar:O_2 (99.5:0.5), corresponding to an oxygen potential of about −420 kJ mol^{-1}, which is required to prepare un-doped, UO_2 at 1600 °C, with a deviation from stoichiometry smaller than 0.0005 [14, 15]. The temperature was hold for 2 h before it was further heated to 1600 °C with 5 °C min^{-1}. An isotherm of 10 h was maintained and at its end the atmosphere was switched back to Ar. Then, the samples

This project has received funding from the EURATOM research and training programme 2014-2018 under grant agreement No 755171. The content of this deliverable reflects only the author's view. The European Commission is not responsible for any use that may be made of the information it contains.

were cooled down to 200 °C with 5 °C min^{-1} and subsequently placed in a desiccator to reach room temperature.

CHARACTERIZATION TECHNIQUES

DETERMINATION OF U, Nd, Ce AND NO^{3-} CONCENTRATION

Metal concentrations of the ADUN solution and the Ce^{III} precursor solutions were determined via ICP-MS. An ELEMENT 2 system (Thermo Scientific) was calibrated with 1 ppb, 2 ppb, 5 ppb, 10 ppb and 20 ppb U and Ce solutions, prepared from 1000 ppm single element standards (SPEX, CertiPrep) diluted with a matrix consisting of ultrapure water and HNO_3 (2 % V/V). A dilution factor of $1:10^8$ was applied to the sample solutions.

In addition, ICP-MS analyses of the dried gels were performed to determine the actual dopant content of the compositions. Two microspheres of each composition (7.8 mg to 13.7 mg) were dissolved in 1 mL HNO_3 , to prepare samples. After dissolution, a volume of 9 mL ultra pure water was added and the solutions were further diluted (1:2000). Moreover, 10 µL of the sol was sampled during the synthesis, which were subsequently mixed with 990 µL dilution matrix. Those samples were further diluted with a factor of 1:5000. The directly measured mass concentrations have a relative uncertainty of 10 % (2σ) and were converted into the molar concentrations to determine the cerium molar metal fraction of each composition.

The molar NO^{3-} concentration of the ADUN solution was estimated, using a relation between the molar U concentration, the density and the NO^{3-} concentration as described by Haas et al. [5], to calculate the $c(NO^{3-})/c(U)$ ratio. The density was determined by pipetting ten times 1.0 mL solution into a beaker and measuring the individual masses on an analytical balance (Mettler-Toledo AT201).

OPTICAL MICROSCOPY (OM)

OM analyses of the dried gels were performed with a HIROX MX-2016Z microscope and a magnification of 100×. Prior to the particle analyses and afterwards, images of a calibration standard were recorded (Keyence OP-88141). A HI-SCOPE Advanced KH-3000 system (HIROX) was used for the data acquisition, and data processing was done using the software package *Fiji* (Version 1.52p) [16].

Five particles of each composition were analysed. The individual particle masses were measured during the sample preparation (Mettler-Toledo AT201). Diameters were measured

This project has received funding from the EURATOM research and training programme 2014-2018 under grant agreement No 755171. The content of this deliverable reflects only the author's view. The European Commission is not responsible for any use that may be made of the information it contains.

in four positions of each particle (90°, 45°, 0° and −45°), which were averaged and the aspect ratio for each particle was determined (d_{max}/d_{min}). Moreover, the average diameter for each individual composition was calculated. Densities were determined, dividing the particle masses by the particle volumes calculated from the diameters, assuming a spherical geometry. The individual densities were also averaged for each composition.

SCANNING ELECTRON MICROSCOPY (SEM)

SEM investigations were carried out to study the shape, morphology and homogeneity of the prepared microspheres, using a Jeol JSM 7100FA field-emission microscope, equipped with a secondary and backscattered electron detector. The working distance ranged from 7 mm to 10 mm and an accelerating voltage of 15 kV was employed. Three sintered particles of each composition were analysed via SEM. The data processing was carried out as described in the previous section for the OM. Diameters and aspect ratios were determined for each particle and average diameters were calculated for the compositions.

X-RAY POWDER DIFFRACTION (XRD)

XRD analyses were carried out using a PANanalytical X'Pert Pro diffractometer. The device utilises a Bragg–Brentano parafocusing geometry in a θ-θ configuration. A sintered, high purity silicon disc was used for zero point calibration. Weekly validations were performed on a sintered alumina disc (NIST Standard Reference Material 1976b). Lattice parameter refinement of silicon was done to assess the instrument bias, which was found to be smaller than 2×10^{-5} relative (2σ). A copper LFF X-ray tube was used as radiation source. The measurement of high-quality diffractograms with low axial divergence was ensured by a combination of a fixed divergence slit, 0.02 rad soller slits and a copper beam mask in the incident beam path.

The sample was mixed with ethanol in a mortar and ground, the resulting suspension was dropped on a zero background silicon single crystal holder. After evaporation of the ethanol, the specimen was mounted into the device and diffractograms were recorded. For the dried gels, a range from 10° to 80° 2θ with a step size of 0.017° 2θ was measured, while the sintered particles were measured in the range from 20° to 143° 2θ, using the same step size.

Lattice parameters were determined using the unit cell refinement option of the software package *HighScore Plus* by PANalaytical (Version 4.8), which applies the method described by Nelson and Riley [17]. For some compositions the presence of two phases was observed, the lattice parameter of those phases were determined applying the Rietveld refinement [18]

This project has received funding from the EURATOM research and training programme 2014-2018 under grant agreement No 755171. The content of this deliverable reflects only the author's view. The European Commission is not responsible for any use that may be made of the information it contains.

option of the same software package. Detailed peak shape analyses of the biphasic compositions' reflections were carried out using the application *Fityk* (Version 0.9.8) [19].

RESULTS AND DISCUSSION

GELATION AND POST-GELATION TREATMENT

Ce-doped microsphes with Ce contents up to 30 mol% were successfully synthesised via internal gelation, using the trivalent dopant precursor. The actual dopant content in the sol ($\chi(\text{dopant})_{sol}$, Table 1) did not deviate significantly from the aimed content ($\chi(\text{dopant})_{aimed}$, Table 1). Intact spheres were obtained and the spherical shape remained during all post gelation steps. No broken particles were observed for any of the compositions.

Table 1.: Ce molar metal fractions determined via ICP-MS in the sol ($\chi(Ce)_{sol}$) and for dissolved particles($\chi(Ce)_{particle}$), as well as diameters of the dried particles (d_{dried} , OM) and sintered particles ($d_{sintered}$, SEM), including the largest aspect ratio of each batch.

Ce precursor	$\chi(Ce)_{aimed}$ / mol%	$\chi(Ce)_{sol}$ / mol%	$\chi(Ce)_{particle}$ / mol%	d_{dried} / mm	aspect ratio	$d_{sintered}$ / mm	aspect ratio
-	0			1.51(3)	1.04	0.78(5)	1.01
Ce^{III}	5	5.1	5.1	1.36(3)	1.02	0.75(5)	1.01
	10	10.1	10.3	1.39(2)	1.01	0.78(4)	1.01
	15	15.4	15.8	1.37(6)	1.02	0.77(5)	1.01
	20	20.4	21.1	1.34(7)	1.05	0.78(1)	1.01
	25	25.7	25.5	1.57(4)	1.02	0.90(1)	1.01
	30	31.8	30.7	1.53(3)	1.04	[a]	
Ce^{IV}	5	4.7	4.8	1.30(2)	1.02	0.88(4)	1.01
	10	9.5	9.6	1.28(2)	1.12	0.88(5)	1.02
	15	14.2	14.4	[b]			
	20	19.9	19.5	[b]			

[a] No diameters determined, since particles broke apart during sintering

[b] No diameters determined, since no spherical geometry was obtained

In the case of the tetravalent Ce precursor, an incomplete gelation was observed for compositions exceeding 5 mol% Ce. For the composition with 10 mol% Ce content, this resulted in a minor fraction of agglomerated spheres, as presented in Figure 2, while for the compositions with 15 mol% and 20 mol% Ce content no spherical shape could be obtained using the chosen parameters. Therefore it was decided to not further increase the Ce content for this precursor.

This project has received funding from the EURATOM research and training programme 2014-2018 under grant agreement No 755171. The content of this deliverable reflects only the author's view. The European Commission is not responsible for any use that may be made of the information it contains.

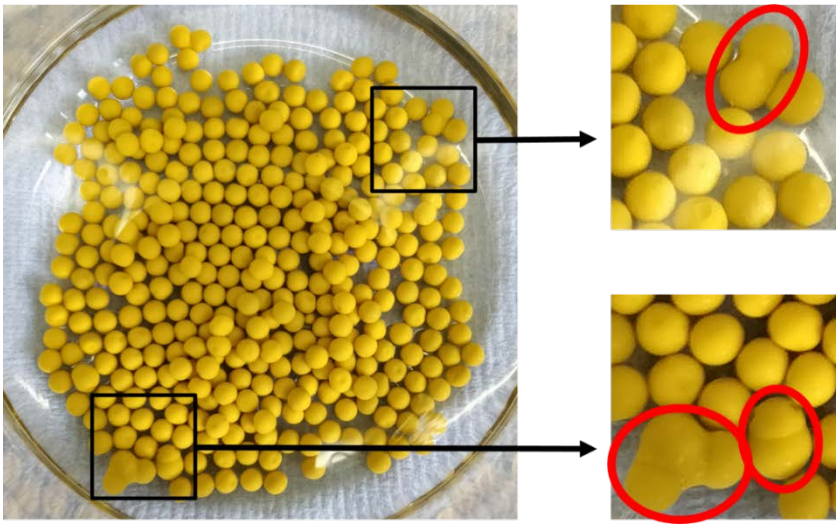

Figure 2.: Agglomerated spheres after the gelation of a sol containing 10 mol% Ce, using CeIV as precursor.

The Ce-doped microspheres prepared with Ce^{III}, changed their colour from yellow to a bright shade of green during the ageing in NH_3 solution. For the Ce-doped compositions prepared with the Ce^{IV} precursor, this colour change did not occur during the washing step, but while drying in air the particles turned into dark-green.

CHARACTERISATION OF DRIED GELS

The relative deviation between the actual dopant content of the dissolved particles ($\chi(Ce)_{particle}$, Table 1) and the aimed dopant content ($\chi(Ce)_{aimed}$, Table 1) ranged for the compounds prepared with the trivalent precursor between 2 % and 5.5 %, while it was ≤ 4 % for the compounds prepared using the tetravalent precursor. The dopant molar metal fractions determined in samples of the sol ($\chi(Ce)_{sol}$, Table 1) exhibit different variations from the aimed dopant content, compared to the contents determined in the dissolved particles ($\chi(Ce)_{particle}$, Table 1). However, all deviations are within the molar metal fractions' uncertainty, allowing us to conclude that no remarkable leaching on one of the metals occurred during the post gelation treatment of the synthesis process.

Micrographs of a dried, un-doped particle and dried Ce doped particles, recorded via OM, are presented in Figure 3 (top). Images of 5 particles per composition were used to determine particle diameters, which were found to range between 1.28(2) mm and 1.89(4) mm for the individual compositions, the results are listed in Table 1. The aspect ratios varied between 1.01 and 1.07 (Table 1). For the composition doped with 10 mol% Ce (Ce^{IV} precursor), a higher aspect ratio was observed (1.12).

This project has received funding from the EURATOM research and training programme 2014-2018 under grant agreement No 755171. The content of this deliverable reflects only the author's view. The European Commission is not responsible for any use that may be made of the information it contains.

Densities of the dried particles, determined by OM, are presented in Figure 4a. For the compositions prepared with the trivalent Ce precursor, a density of 2.44 g cm^{-3} was found for the 5 mol% doped composition, which increased with increasing Ce content, reaching a maximum of 3.00 g cm^{-3} for 20 mol% Ce. For Ce contents of 25 mol% and 30 mol%, a comparable density of 2.73 g cm^{-3} and 2.76 g cm^{-3} was determined. The usage of the tetravalent Ce precursor led to gels with a higher density than those prepared with Ce^{III} (Figure 4a). Values of 3.23 g cm^{-3} and 3.45 g cm^{-3} were determined for the 5 mol% and 10 mol% Ce-doped compositions, respectively. Since only those compositions could be fabricated maintaining a spherical shape, there are only two data-points for this series are included in the plot.

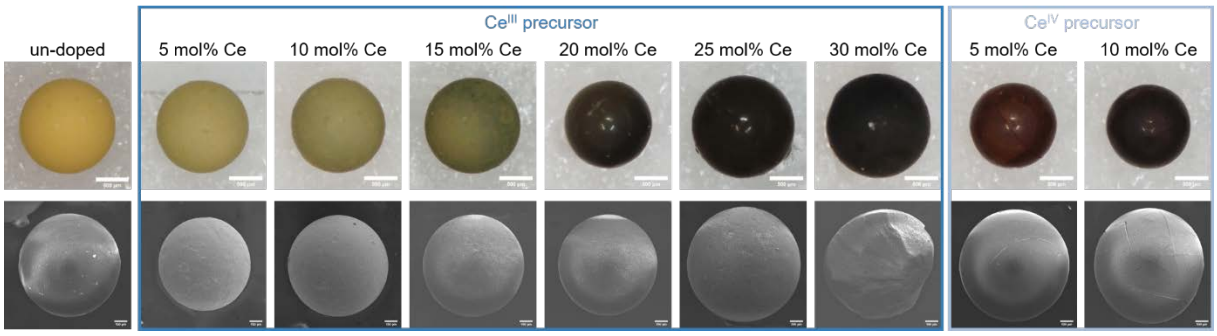

Figure 3.: Images of the dried gels (top), taken via optical microscopy, as well as SEM micrographs of the sintered particles (bottom).

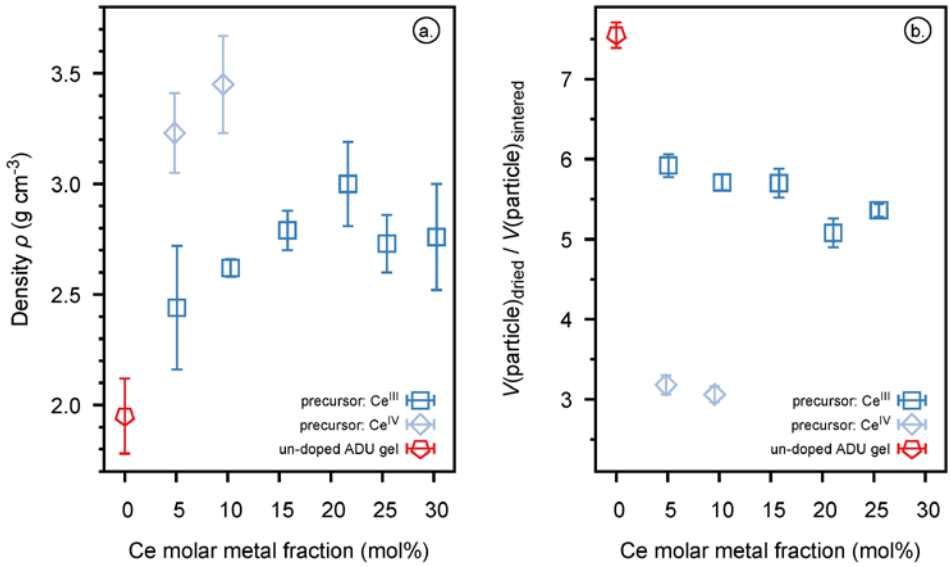

Figure 4.: Densities of dried gels (a.), and volume of dried particles, derived from OM, standardised to volume of sintered particles, derived from SEM, (b.). The uncertainties are given with a confidence level of 2σ.

This project has received funding from the EURATOM research and training programme 2014-2018 under grant agreement No 755171. The content of this deliverable reflects only the author's view. The European Commission is not responsible for any use that may be made of the information it contains.

Figure 5 shows the XRD pattern obtained for the dried un-doped microspheres (bottom) and those of the Ce doped particles. The un-doped material was identified as ADU with $3UO_3 \cdot 2NH_3 \cdot 4H_2O$ stoichiometry [20] and its diffractogram looks, apart from obvious intensity variations, comparable to one of the Ce-doped compositions prepared with Ce^{III}. The XRD patterns of the Ce-doped compositions show a significantly different degree of crystallinity for the different Ce precursors. For the compositions prepared with Ce^{IV}, a remarkably lower peak-to-background ratio can be observed, indicating large fractions of an amorphous phase (Figure 5). However, for all Ce-doped compositions no additional reflections compared to the un-doped material can be observed. A close inspection of the diffractograms reveals a shift of the reflections to higher 2θ angles with increasing Ce content for both dopant precursors, indicating a lattice contraction that might be caused by the incorporation of the dopant into the ADU matrix.

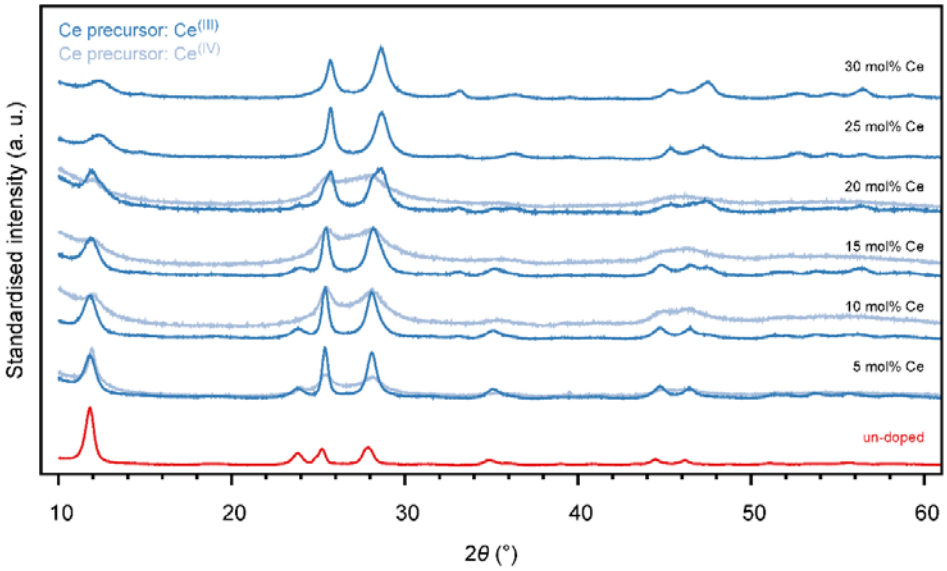

Figure 5.: XRD pattern of the dried un-doped gel (a.) and dried gels doped with Ce, prepared using Ce^{III} and Ce^{IV} precursors.

THERMAL TREATMENT

The particles' spherical shape for all compositions, prepared using the trivalent Ce precursors, was maintained during the calcination at 900 °C in air and no broken microspheres were observed. Moreover, no significant shrinkage of the particles took place within the treatment.

During the sintering in reducing conditions at 1600 °C for 10 h, the un-doped particles and all Nd-doped particles remained in their spherical shape. For the compositions containing 20

This project has received funding from the EURATOM research and training programme 2014-2018 under grant agreement No 755171. The content of this deliverable reflects only the author's view. The European Commission is not responsible for any use that may be made of the information it contains.

mol% and 25 mol% Ce (Ce^{III} precursor), a remarkable fraction of broken particles was observed, while for the 30 mol% Ce composition only a negligible amount of spheres was retained. All compositions underwent a significant shrinkage within this step. Figure 4b shows the ratios of the dried particles' volume and the sintered particles' volume. The volumes were calculated using diameters determined via OM for the dried particles and by SEM for the sintered particles (Table 1). We can observe significant shrinkage variations for the different compounds prepared within this study. The volume of the dried, un-doped particles was found to be 7.55 times higher than the volume of the sintered, un-doped particles. The Ce-doped compositions prepared with Ce^{III} decreased in volume, in the range of 5 to 6 during the thermal treatment, while the compositions prepared using Ce^{IV} showed a shrinkage factor of about 3.1.

CHARACTERIZATION OF SINTERED MICROSPHERES

SEM micrographs of un-doped and Ce-doped microspheres are shown in Figure 2 (bottom). Diameters of the microspheres were measured and ranged between 750(50) µm and 900(10) µm for the individual compositions. The largest aspect ratio of each individual batch was found to range between 1.01 and 1.02, proving the spherical shape of the microspheres. The results of those calculations are included in Table 1. However, for the Ce-doped particles prepared with the tetravalent Ce precursor, a large amount of cracks on the particles' surface was observed, which was not the case for the particles prepared using Ce^{III}, but close-ups of the surfaces showed grains with neither intergrain nor intragrain pores in the material.

Figure 6 illustrates the XRD pattern of the sintered un-doped microspheres (bottom) and those of the Ce doped particles. The XRD data were used to determine lattice parameters for the individual compositions. The Cu $K_{\alpha 1}$ wavelength of 1.5405929 Å [21] was used, and a small correction for the temperature difference of the samples with respect to a reference value of 20 °C was applied [15]. For the latter, the UO_2 thermal expansion coefficient published by Fink [22] was used. The results are plotted as function of the Ce molar metal fraction in Figure 7.

This project has received funding from the EURATOM research and training programme 2014-2018 under grant agreement No 755171. The content of this deliverable reflects only the author's view. The European Commission is not responsible for any use that may be made of the information it contains.

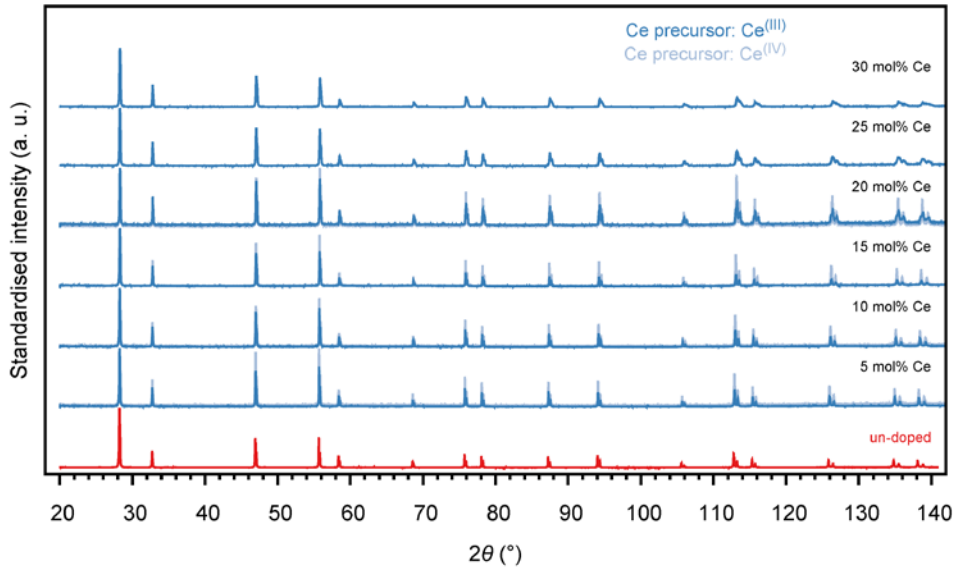

Figure 6.: XRD pattern of un-doped UO_2 particles (bottom) and products doped with Ce, prepared using Ce^{III} and Ce^{IV} precursors.

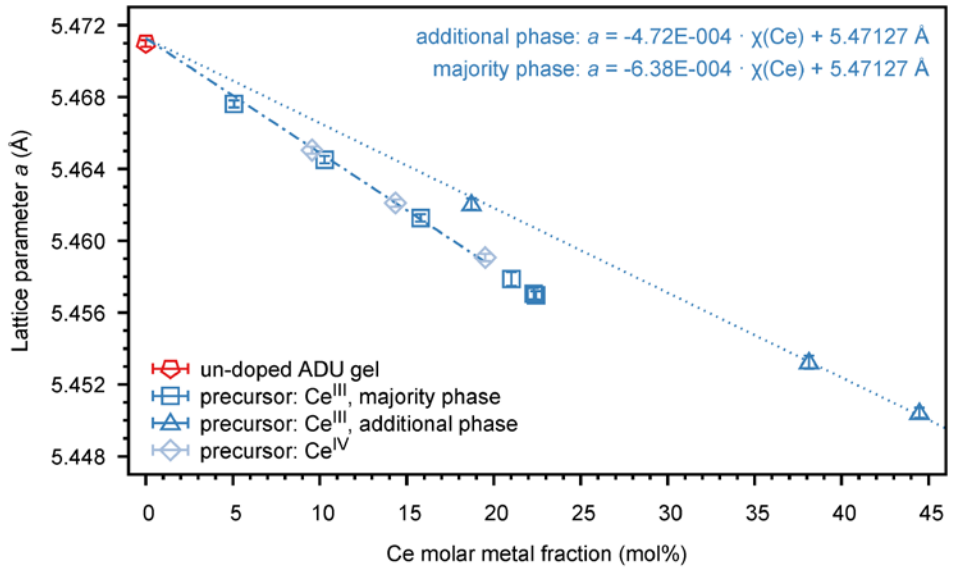

Figure 7.: Lattice parameter *a* as function of Ce molar metal fraction for the sintered microspheres, and a linear fit through an intercept corresponding to the lattice parameter of stoichiometric UO_2 [15]. The uncertainties are given with a confidence level of 2σ.

This project has received funding from the EURATOM research and training programme 2014-2018 under grant agreement No 755171. The content of this deliverable reflects only the author's view. The European Commission is not responsible for any use that may be made of the information it contains.

A lattice parameter of 5.4710(2) Å was determined for the un-doped material at 20 °C. The result is marginally smaller, than the UO_2 lattice parameter published by Leinders et al. [15] (5.4713(2) Å at 20 °C), but the uncertainty intervals overlap, allowing us to conclude that the material represents a UO_2 phase.

For the compositions prepared with the Ce^{IV} precursor, a linearly decreasing lattice parameter with increasing Ce content was observed. The compositions prepared with Ce^{III} precursor behave similarly for a Ce content up to 15 mol%. For the mentioned compositions, the slope of the linear function was determined by a linear fit constrained at 0 mol% dopant level to intercept with the lattice parameter of stoichiometric UO_2 at 20 °C (5.4713(2)Å) [15]. A slope of $-6.38(7) \times 10^{-4}$ with a R^2 of 0.949 was determined (Figure 7, dashdotted line).

Detailed analyses of the diffractograms revealed that the samples prepared using the trivalent precursor with Ce contents above 15 mol% are not monophasic. A magnification of the (026) reflection is exemplarily shown for the compositions containing ≥ 15 mol% Ce (Ce^{III} precursor) in Figure 8. In the case of the 15 mol% Ce-doped composition, this reflection could be fitted with a Pseudo-Voigt function for each of the $K_{\alpha1}$ and $K_{\alpha2}$ peaks (Figure 8a), leading to the red line which describes the experimental data points very well. For the compositions with ≥ 20 mol% Ce, two further Pseudo-Voigt functions (orange lines) had to be introduced (Figure 8b-d), leading to sums (black lines) which match the experimental data points and indicate that those compositions are biphasic.

In order to quantify the weight fractions corresponding to each phase, Rietveld refinements were performed with the following assumptions: (1) two $U_{1-y}Ce_yO_2$ phases are considered, both assuming an ideal fluorite structure ($Fm\bar{3}m$), (2) the Ce content y in each phase is fixed at the nominally aimed molar metal fraction, i.e. 0.20, 0.25, 0.30. One might expect to have different Ce contents in both phases, however, the effect on the diffracted intensity is only marginal even when an uncertainty interval of the order $y = \pm 0.1$ is considered. Hence the weight fractions attributed to each phase are hardly affected by their actual Ce content. Owing to the sample preparation used for XRD (i.e. pipetting of a suspension on a zero-background holder, see materials and methods on p. 7) the pattern presents a high degree of preferential orientation. Additionally, because only a thin layer of powder is applied to the holder, the diffracting volume will vary between low and high diffraction angles, which affects the scattered intensity. To avoid this divergence, the Rietveld refinement was restricted to the range 83° to 143° 2θ, which is also the region most sensitive to probing peak shifts due to variations in lattice parameter. The refinement parameter set consisted of a cubic Chebyshev polynomial to model the background, the scale factor and lattice parameter of both phases along with a global parameter for sample displacement, and two Pseudo Voigt functions.

This project has received funding from the EURATOM research and training programme 2014-2018 under grant agreement No 755171. The content of this deliverable reflects only the author's view. The European Commission is not responsible for any use that may be made of the information it contains.

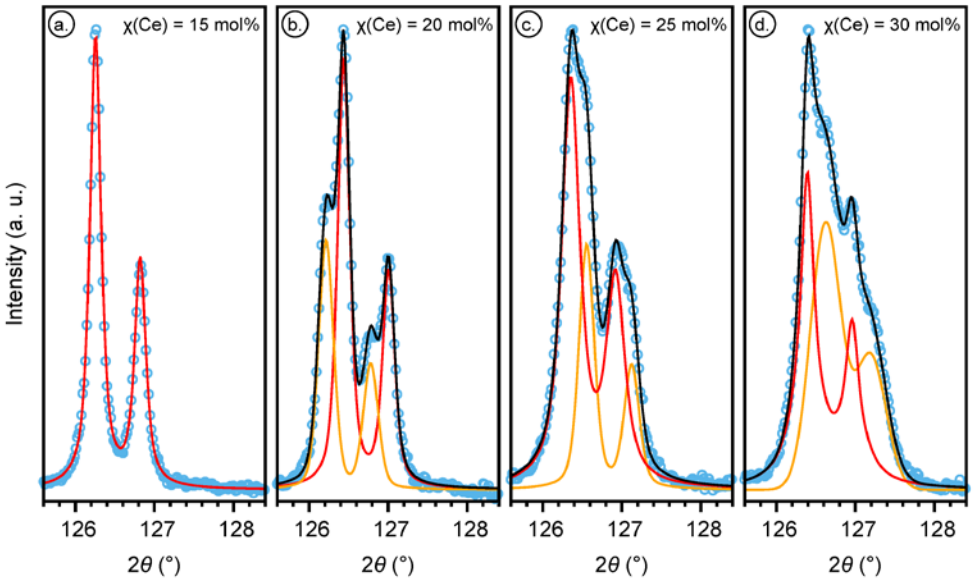

Figure 8.: XRD data of sintered microspheres with χ(Ce) ≥ 15 mol%, prepared using Ce^{III}, for the 2θ range from 125.6° to 128.4° (reflection with hkl equals 026), and Pseudo-Voigt fits for the main phase (red), the additional phase (orange) and their sum (black).

The Rietveld refinement revealed for all affected compositions main phases (64 wt% to 75 wt%) having similar lattice parameters (5.4570(2) Å, 5.4579(4) Å and 5.4570(3) Å), indicating a solubility limit for Ce incorporation under the applied conditions. Based on the lattice parameters, the expected Ce content was calculated using the linear relation found for the single phase Ce-doped samples (da/dy = −6.38(7)×10^{-4}, R^2 = 0.908, Figure 7). Ce molar metal fractions of 22.4 mol%, 21.0 mol% and 22.3 mol% were determined. From those values, the known total Ce-content ($\chi(Ce)_{particle}$, Table 1), and the weight fraction attributed to each phase, the Ce content in the additional phase can be derived. The lattice parameters of the additional phases (5.4620(3) Å, 5.4532(4) Å and 5.4504(3) Å) are plotted as function of the resulting Ce molar metal fractions (18.7 mol%, 38.1 mol% and 44.5 mol%) in Figure 7 as well. The additional phase, present in the biphasic compositions, depends linearly on the Ce content (da/dy = −4.71(5)×10^{-4}, R^2 = 0.952, Figure 7, dotted line). The slope is significantly larger than the one observed for the main phase. Antonio et al. [23] did not observe a signal at the XANES absorption edge of $U_{0.33}Ce_{0.67}O_2$ (Ce: L_3 -edge, U: M_5 -edge), associated with Ce^{III} , nor any anomalous signal which could be associated with anything but U^{IV}. Thus, we assume that those increased lattice parameters are caused by an incomplete oxidation of Ce^{III} during the calcination, or by a partial reduction of Ce^{IV} to Ce^{III}, as described by Ha et al. [24]. This also explains the fact that the microspheres with biphasic compositions did not remain in the spherical shape and broke apart during the sintering under reducing conditions.

This project has received funding from the EURATOM research and training programme 2014-2018 under grant agreement No 755171. The content of this deliverable reflects only the author's view. The European Commission is not responsible for any use that may be made of the information it contains.

A comparison of the lattice parameter obtained for the Ce-doped material is presented in Figure 9. The experimental lattice parameters of this study for Ce dopant contents below the solubility limit of 22.4 mol% agree well to reference data [25-27] (Figure 9). The reference material was prepared by solid-state synthesis and co-precipitation [25], but also a citrate combustion method [26, 27] was applied. The obtained powders were pelletized and sintered in Ar/H_2 mixtures with H_2 contents of 5 % or 8 %, equilibrated with water at 0 °C or 5 °C, the sintering temperatures ranged between 800 °C and 1450 °C. Even though a remarkably lower sintering temperature was applied, Venkata Krishnan et al. [26] and Sali et al. [27] obtained single phase solid solutions for compositions with Ce contents > 22.4 mol%, following the trend we observed for the main phase in our samples.

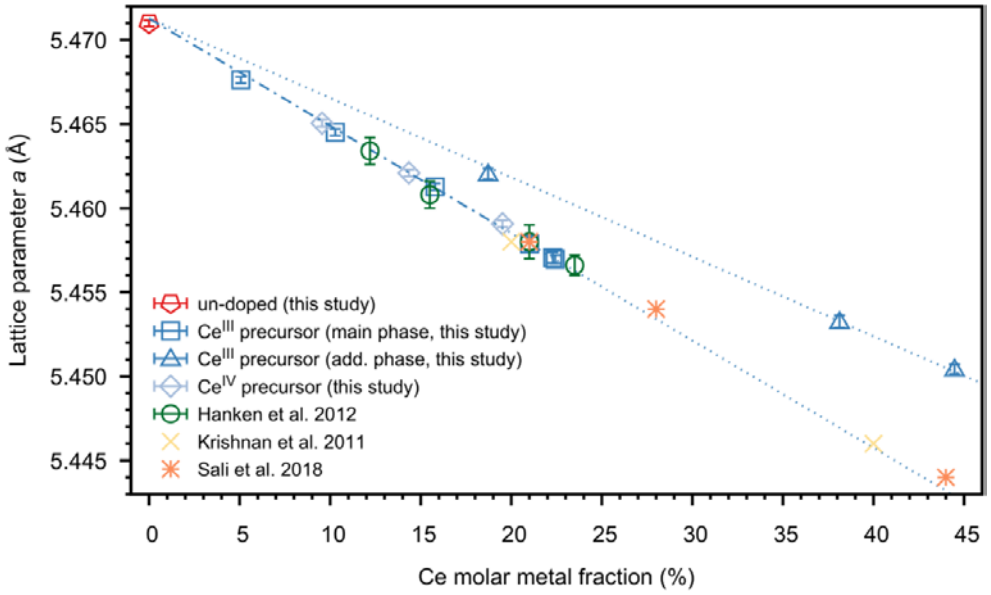

Figure 9: Lattice parameter a as function of the Ce molar metal fraction of the sintered, Ce-doped microspheres, compared to reference data [25-27]. The uncertainties are given with a confidence level of 2σ.

This project has received funding from the EURATOM research and training programme 2014-2018 under grant agreement No 755171. The content of this deliverable reflects only the author's view. The European Commission is not responsible for any use that may be made of the information it contains.

CONCLUSION

Ce-doped microspheres with a good sphericity and dopant contents up to 30% were successfully synthesized via internal gelation, using trivalent Ce precursors, while an incomplete gelation was observed for gels prepared with Ce^{IV} precursors and Ce contents of ≥ 15 mol%. The density of the dried gels depends not only on the gelation conditions but also on the dopant and the oxidation state of its precursor. The density for Ce-doped gels was found to be higher than the one of un-doped particles, prepared with the same parameter. The usage of Ce^{IV} as precursor led to gels with higher densities than those prepared with Ce^{III}. The XRD patterns of the dried gels indicate a successful introduction of the dopant into the $3UO_3 \cdot 2NH_3 \cdot 4H_2O$ matrix, independent of the oxidation state of its precursor. The shrinkage during the thermal treatment for gels prepared with the Ce^{IV} precursors are about a factor of 0.5 smaller than the ones of the microspheres prepared with Ce^{III}. XRD analyses proved the presence of $U_{1-y}Ce_yO_2$ single phase solid solutions for the sintered Ce-doped particles (Ce^{IV} precursor). For Ce-doped compositions prepared using the trivalent precursor, two solid solutions were observed for Ce contents > 15 mol%, which relates to the physical stability of those sintered particles, i.e. the large fraction of broken particles during the thermal treatment. The lattice parameters determined for the single phase solid solutions follow Vegard's law and show a decreasing lattice parameter with increasing dopant content. The gelation and thermal treatment conditions investigated in this study are suitable for the preparation of $U_{1-y}Ce_yO_2$ single phase solid solutions with Ce molar metal fractions up to 15 mol%, using cerium(III) nitrate hexahydrate as dopant precursors.

This project has received funding from the EURATOM research and training programme 2014-2018 under grant agreement No 755171. The content of this deliverable reflects only the author's view. The European Commission is not responsible for any use that may be made of the information it contains.

REFERENCES

[1] D. Lundberg, I. Persson, The size of actinoid(III) ions – structural analysis vs. common misinterpretations, Coordination Chemistry Reviews 318 (2016) 131-134.

[2] R.D. Shannon, Revised effective ionic radii and systematic studies of interatomic distances in halides and chalcogenides, Acta Crystallographica Section A: Crystal Physics, Diffraction, Theoretical and General Crystallography 32(5) (1976) 751-767.

[3] F.W. Van Der Brugghen, M.E.A. Hermans, J.B.W. Kanij, A.J. Noothout, T. Van Der Plas, H.S.G. Slooten, Sol-gel processes for the preparation of spherical thorium-containing fuel particles, Keuring van Electrotechnische Materialen, NV, Arnhem (Netherlands), 1968.

[4] R. Förthmann, Die chemischen Grundlagen des Hydrolyseverfahrens zur Herstellung sphärischer Kernbrennstoffteilchen, Kernforschungsanlage Jülich German1973.

[5] P.A. Haas, J.M. Begovich, A.D. Ryon, J.S. Vavruska, Chemical flowsheet conditions for preparing urania spheres by internal gelation, United States, 1979, p. 73.

[6] R.D. Hunt, J.L. Collins, Uranium kernel formation via internal gelation, Radiochimica Acta 92(12/2004) (2004) 909-915.

[7] V.N. Vaidya, Status of sol-gel process for nuclear fuels, Journal of Sol-Gel Science and Technology 46(3) (2008) 369-381.

[8] S. Li, J. Bai, S. Cao, X. Yin, C. Tan, P. Li, W. Tian, J. Wang, H. Guo, Z. Qin, An improved internal gelation process without cooling the solution for preparing uranium dioxide ceramic microspheres, Ceramics International 44(2) (2018) 2524-2528.

[9] M.A. Pouchon, G. Ledergerber, F. Ingold, K. Bakker, Sphere-Pac and VIPAC Fuel, in: R.J.M. Konings (Ed.), Comprehensive Nuclear Materials, Elsevier BV, Oxford, 2012, pp. 275-312.

[10] S. Suryanarayana, N. Kumar, Y.R. Bamankar, V.N. Vaidya, D.D. Sood, Fabrication of UO_2 pellets by gel pelletization technique without addition of carbon as pore former, J Nucl Mater 230(2) (1996) 140-147.

[11] V.N. Vaidya, S.K. Mukherjee, J.K. Joshi, R.V. Kamat, D.D. Sood, A study of chemical parameters of the internal gelation based sol-gel process for uranium dioxide, J Nucl Mater 148(3) (1987) 324-331.

[12] A. Kumar, J. Radhakrishna, N. Kumar, R.V. Pai, J.V. Dehadrai, A.C. Deb, S.K. Mukerjee, Studies on preparation of (U_0.47,Pu_0.53)O_2 microspheres by internal gelation process, J Nucl Mater 434(1) (2013) 162-169.

[13] I. Grenthe, J. Drożdżyński, T. Fujino, E.C. Buck, T.E. Albrecht-Schmitt, S.F. Wolf, Uranium, in: L.R. Morss, N.M. Edelstein, J. Fuger (Eds.), The Chemistry of the Actinide and Transactinide Elements, Springer Netherlands, Dordrecht, 2006, pp. 253-698.

[14] T.B. Lindemer, T.M. Besmann, Chemical thermodynamic representation of $UO_{2\pm x}$, J Nucl Mater 130 (1985) 473-488.

[15] G. Leinders, T. Cardinaels, K. Binnemans, M. Verwerft, Accurate lattice parameter measurements of stoichiometric uranium dioxide, J Nucl Mater 459 (2015) 135-142.

This project has received funding from the EURATOM research and training programme 2014-2018 under grant agreement No 755171. The content of this deliverable reflects only the author's view. The European Commission is not responsible for any use that may be made of the information it contains.

[16] J. Schindelin, I. Arganda-Carreras, E. Frise, V. Kaynig, M. Longair, T. Pietzsch, S. Preibisch, C. Rueden, S. Saalfeld, B. Schmid, J.-Y. Tinevez, D.J. White, V. Hartenstein, K. Eliceiri, P. Tomancak, A. Cardona, Fiji: an open-source platform for biological-image analysis, Nature Methods 9(7) (2012) 676-682.

[17] J.B. Nelson, D.P. Riley, An experimental investigation of extrapolation methods in the derivation of accurate unit-cell dimensions of crystals, Proceedings of the Physical Society 57(3) (1945) 160-177.

[18] H. Rietveld, A profile refinement method for nuclear and magnetic structures, Journal of Applied Crystallography 2(2) (1969) 65-71.

[19] M. Wojdyr, Fityk: a general-purpose peak fitting program, Journal of Applied Crystallography 43(5 Part 1) (2010) 1126-1128.

[20] C. Schreinemachers, G. Leinders, G. Modolo, M. Verwerft, K. Binnemans, T. Cardinaels, The conversion of ammonium uranate prepared via sol-gel synthesis into uranium oxides, Nuclear Engineering and Technology (2019).

[21] J. Härtwig, G. Hölzer, E. Förster, K. Goetz, K. Wokulska, J. Wolf, Remeasurement of characteristic X-ray emission lines and their application to line profile analysis and lattice parameter determination, 143(1) (1994) 23-34.

[22] J.K. Fink, Thermophysical properties of uranium dioxide, J Nucl Mater 279(1) (2000) 1-18.

[23] M.R. Antonio, U. Staub, J.S. Xue, L. Soderholm, Comparison of the Cation Valence and Coordination in Ce_2UO_6 and Ce_2MoO_6, Chemistry of Materials 8(11) (1996) 2673-2680.

[24] Y.-K. Ha, J. Lee, J.-G. Kim, J.-Y. Kim, Effect of Ce doping on UO_2 structure and its oxidation behavior, J Nucl Mater 480 (2016) 429-435.

[25] B.E. Hanken, T.Y. Shvareva, N. Grønbech-Jensen, C.R. Stanek, M. Asta, A. Navrotsky, Energetics of cation mixing in urania–ceria solid solutions with stoichiometric oxygen concentrations, Physical Chemistry Chemical Physics 14(16) (2012) 5680-5685.

[26] R. Venkata Krishnan, G. Panneerselvam, B.M. Singh, B. Kothandaraman, G. Jogeswararao, M.P. Antony, K. Nagarajan, Synthesis, characterization and thermal expansion measurements on uranium–cerium mixed oxides, J Nucl Mater 414(3) (2011) 393-398.

[27] S.K. Sali, M. Keskar, R. Phatak, K. Krishnan, G.P. Shelke, P.P. Muhammed Shafeeq, S. Kannan, Oxidation behavior of $(U_{1-y}Ce_y)O_{2.00}$; (y = 0.21, 0.28 and 0.44) solid solutions under different oxygen potentials. Thermogravimetric and in situ X-ray diffraction studies, J Nucl Mater 510 (2018) 499-512.

This project has received funding from the EURATOM research and training programme 2014-2018 under grant agreement No 755171. The content of this deliverable reflects only the author's view. The European Commission is not responsible for any use that may be made of the information it contains.